2018 European Control Conference (ECC)
June 12-15, 2018. Limassol, Cyprus

Automatic Notch Filter Width Tuning for Resonance Peaks in Gearless Servo Drives

Mario Aldag, Joachim Horn
Institute of Control Engineering, Department of Electrical Engineering
Helmut-Schmidt-University/University of the Federal Armed Forces Hamburg
Holstenhofweg 85, 22043 Hamburg, Germany
Email: mario.aldag@hsu-hh.de

***Abstract*—The performance of a gearless servo system is significantly degraded by mechanical resonances present in the system. For applications on a machine the parameters of the mechanical resonances differ from workpiece to workpiece and thus cannot be calculated a priori. The use of notch filters is a common approach to dampen these resonances. This paper introduces a novel, fast and resource efficient algorithm capable of estimating the width of a notch filter. The performance of this algorithm is validated with a MATLAB simulation with datasets from two different machines. After the notch filter has been appropriately designed, it is shown the controller gains could be increased to improve the overall tracking performance.**

I. Introduction

Servo motors are commonly used in industrial fields such as robotics or machines. An industrial system using a servo motor usually includes several other parts, for example a frequency inverter, a gear, an encoder and a mechanical plant.

Regarding machines, workpieces can be mounted on a round table. They typically cannot be treated as an endlessly stiff connection to the motor due to high gains in the controller. Thus, the mechanical plant includes an elastic coupled load which will lead to resonances in the machine and thus degrade the performance, because it can lead to high position tracking errors.

The traditional servo motor system includes a gear. When direct drives are used no gear is present in the system. This leads to an increased impact of mechanical resonances in the control system, thus increasing the demand to dampen those resonances. In machines different workpieces shall be processed which results in different plant settings (masses, stiffnesses and dampings). The plant characteristic is typically a two- or three-mass system.

Unknown resonances require a robust control design. The most common way is to reduce the controller gains which will lead to poor tracking performance. Another common control optimization attempt is the direct identification of mechanical resonances without generating a parametrized plant model. If the mechanical resonance parameters can be identified (mainly resonance frequency and damping), a notch filter can be used to dampen the resonance. This has been shown in [1]. The main benefit of this approach is that no a priori knowledge of the plant is needed. [2] has compared the impact of PI, 2-DOF PI with fixed notch filters and neural network controller on control performance with unknown resonances present in the system.

[3] has already discussed different frequency identification algorithms ([4], [5], [6]). [7] gives a good overview of different methods to dampen vibrations with adaptive regulations. [3] has proposed a modified "Scanning-Algorithm" based on [8] which uses a bandpass to scan the frequency response of a signal. This method was used in [9] to detect multiple resonance peaks present in the spectrum in real time implemented on a digital signal processor and will also be used in this paper to identify and dampen the resonance.

To identify the plant, this paper uses a time domain approach with an invasive signal. Due to the change in the workpiece an identification run can be processed prior manufacturing. Invasive time domain signals have already widely been used ([10], [11], [12]) for several applications.

Most recent studies about adaptive notch filters were also carried out by [13], [14] or [15]. All of them dealed with different aspects, such as notch filter depth tuning or loop analysis. This paper introduces a novel algorithm capable of estimating the necessary notch filter with for an automatic identification. This parameter is especially important in the dynamic region of the controller, because the notch filter will introduce an additional phase lag prior to the resonance frequency. This phase lag increases as the width gets bigger, thus it is especially important to keep the notch filter width to a minimum. Especially [16] has analyzed the influence of additional notch filter in closed loop control architectures using an equivalent Frequency locked loop (FLL) model.

Section II gives an overview of the used system and used signals, which will be simulated in Section III. Section IV introduces the novel algorithm capable to estimate a notch filter width in an efficient manner. A simulation of the algorithm will be shown in Section V.

II. System Modeling

The control system consists of three cascaded PI controllers for current, speed and position. The position and speed feedback will be generated from an encoder attached to the torque drive. Therefore the mechanical resonances will mainly be seen on the position and derived speed feedback.

Figure 1 shows a simplified block diagram of the used control system. The position reference φ_r will be generated

by a software shipped with the machine. The measured position φ_M ('M' as motor position) describes the actual position of the round table seen at the motor side, which will be fed into the position controller $G_\mathrm{R1}(s)$. The variable $\dot{\varphi}_\mathrm{M}$ describes the actual speed, u is the output of the speed PI controller $G_\mathrm{R2}(s)$ and I_r^q describes the current reference.

The superscript 'q' is typically used in field-oriented current control topology, which is used in this paper, and denotes the current perpendicular to the motor field. This current is approximately proportional to the resulting motor torque assuming the current in field orientation I_r^d is regulated to zero. Thus, an additional controller for I_r^d is used, but neglected in the block diagram for the sake of simplicity. Parasitic electrical effects such as cogging and reluctance are neglected. The system can dampen resonances in the current reference signal statically with the block called $G_\mathrm{N1}(s)$ as seen in Equation 1.

$$G_\mathrm{N1,2}(s) = \frac{s^2 + g\Delta\omega\,\omega_\mathrm{Res}s + \omega_\mathrm{Res}^2}{s^2 + \Delta\omega\,\omega_\mathrm{Res}s + \omega_\mathrm{Res}^2} \tag{1}$$

The adjustable Notch filter $G_\mathrm{N2}(s)$ includes three parameters: Resonance frequency ω_Res, bandwidth $\Delta\omega$ and depth g. Resonance frequency and depth have already been discussed in [3] and [9], the bandwidth $\Delta\omega$ will be developed in this paper.

For the sake of simplicity the plant $G_\mathrm{S}(s)$ includes the current controller, the electrical plant (from current to a mechanical moment in the motor) and the mechanical plant (motor moment to position). All parts of the plant shall be treated as linear systems, the electrical shall also be time invariant. It follows:

$$G_\mathrm{S}(s) = G_\mathrm{el}(s) \cdot G_\mathrm{M}(s) \tag{2}$$

The transfer function $G_\mathrm{M}(s)$ describes the mechanical part of the plant which will be explained in the next section. The electrical part of the plant uses the current reference I_r^q to generate a motor moment M_M and can be described as:

$$G_\mathrm{el}(s) = \frac{M_\mathrm{M}(s)}{I_\mathrm{r}^\mathrm{q}(s)} = \frac{k_\mathrm{f}}{T_\mathrm{e}s + 1} \tag{3}$$

The parameter k_f is a motor constant and can be derived from the motor datasheet, T_e is the equivalent time constant of the current cascade loop, which is typically $T_\mathrm{e} \approx 2T_\mathrm{t}$ with T_t being the power converter time constant. For in depth analysis of modeling the electric PMSM-machine see [17].

A. Mechanical Multi-Mass System

The mechanical part of the plant is mainly an double-integrating-system with an elastic load. The motor moment $M_\mathrm{M}(s)$ will then be integrated with the inertia of the system Θ to the speed $\dot{\varphi}$ and position φ.

Based on [18] the mechanical two-mass system can be described as a MIMO system:

$$\begin{bmatrix}\dot{\varphi}_\mathrm{A}(s)\\ \dot{\varphi}_\mathrm{M}(s)\end{bmatrix} = \begin{bmatrix}G_\mathrm{AA}(s) & G_\mathrm{MA}(s)\\ G_\mathrm{AM}(s) & G_\mathrm{MM}(s)\end{bmatrix}\begin{bmatrix}M_\mathrm{A}(s)\\ M_\mathrm{M}(s)\end{bmatrix} \tag{4}$$

The transfer function $G_\mathrm{MM}(s)$ denotes the motor side speed $\dot{\varphi}_\mathrm{M}(s)$ with respect to the motor side torque $M_\mathrm{M}(s)$ and

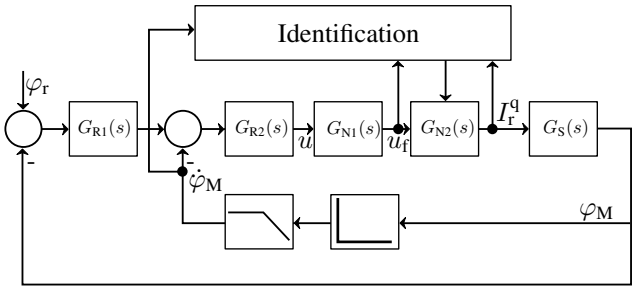

Fig. 1. Block Diagram of the Control System. The control system implements cascaded PI-controllers. The plant includes the current controller and the mechanical plant.

the transfer function $G_\mathrm{AM}(s)$ denotes the motor side speed $\dot{\varphi}_\mathrm{M}(s)$ with respect to the load side torque $M_\mathrm{A}(s)$. The former is the plant in this application, whereas the latter can be used to model the effect of an applied disturbance torque to the motor side speed. Using [17] leads to:

$$G_\mathrm{MA}(s) = \frac{\dot{\varphi}_\mathrm{A}(s)}{M_\mathrm{M}(s)} = \frac{1}{s(\Theta_\mathrm{M}+\Theta_\mathrm{A})} \cdot \frac{1+\frac{d}{c}s}{1+\frac{d}{c}s+\frac{\Theta_\mathrm{M}\cdot\Theta_\mathrm{A}}{c(\Theta_\mathrm{M}+\Theta_\mathrm{A})}s^2} \tag{5}$$

$$G_\mathrm{MM}(s) = \frac{\dot{\varphi}_\mathrm{M}(s)}{M_\mathrm{M}(s)} = \frac{1}{s(\Theta_\mathrm{M}+\Theta_\mathrm{A})} \cdot \frac{1+\frac{d}{c}s+\frac{\Theta_\mathrm{A}}{c}s^2}{1+\frac{d}{c}s+\frac{\Theta_\mathrm{M}\cdot\Theta_\mathrm{A}}{c(\Theta_\mathrm{M}+\Theta_\mathrm{A})}s^2} \tag{6}$$

The system parameters d and c will be derived in the next section, the motor inertia Θ_M can be obtained from the motor datasheet whereas the load inertia Θ_A significantly depends on the mounted workpiece. The transfer functions G_AA and G_AM will not be used in this paper and can be found in [18].

B. Modeling Peaks in Control Plants

Assuming the control plant is modeled as a multi-mass system, multiple resonance peaks are present in the system. In a typical machine further mechanical resonances exist and can be observed.

The common way to represent a resonance capable system $G(s)$ with resonance frequency ω_0 and damping D can be described as:

$$G(s) = \frac{1}{1+2\frac{D}{\omega_0}s+\frac{1}{\omega_0^2}s^2} \tag{7}$$

The quality factor Q can be used to describe the bandwidth B of the resonance peak seen in the transfer function of $G(s)$.

$$Q = \frac{1}{2D} \tag{8}$$

$$B = \frac{\omega_0}{Q} = 2D\omega_0 \tag{9}$$

In a real application the damping D and resonance frequency ω_0 could be measured. Nevertheless, also datasheet parameters from a spring-mass systems with spring constant c_{12}, damper constant d_{12} and load inertia Θ_M could be used.

Using these parameters the following identities could be used:

$$\omega_0 = \sqrt{\frac{c_{12}}{\Theta_\mathrm{A}}} \tag{10}$$

$$D = \frac{d_{12}\,\omega_0}{2c_{12}} \tag{11}$$

Mechanical resonances besides the multi-mass resonances are typically weakly damped and are visible as a sharp peak in a bode diagram of a system or spectrum of a signal. Thus, it is viable to use a small frequency step size for the identification, e.g. 5 Hz.

Since the plant contains an open integrator, mechanical resonances ocurring at high frequencies are naturally damped. Nevertheless, they can deteriorate the controller performance and have to be detected as well as mechanical resonance frequencies occurring at lower frequencies (e.g. $f_\mathrm{Res} < 1000\,\mathrm{Hz}$).

III. Simulation of System

TABLE I. Parameter values for Simulation in SIMULINK

Parameter	Value
Θ_M	$1\,\mathrm{kgm}^2$
Θ_A	$1.13\,\mathrm{kgm}^2$
k_f	$500\,\frac{\mathrm{N}}{\mathrm{A}}$
T_e	$1 \times 10^{-4}\,\mathrm{s}$
ω_0	$2\pi\,800\,\mathrm{Hz}$
D	1×10^{-4}

The simulation will be carried out in MATLAB and SIMULINK. The system shown in Figure 1 will be modeled in SIMULINK. Table I shows the used parameters for the simulation and Figure 2 shows the different transfer functions of the system with closed loop speed control. The ocherous colored graph represents the tracking transfer function in closed loop speed control for an rigid coupled plant. The red and blue colored graphs represent the tracking transfer function in closed loop speed control with an elastic coupled load with respect to the motor (red) or load (blue) side. Figure 3 shows two additional resonances in the red and ocherous colored graph disturbing the system and the blue colored graph represents the designed notch filter, which has previously been identified.

The resonances can be either seen in the actual motor speed $\dot{\varphi}_\mathrm{M}$ or speed controller output u. Throughout this paper the actual motor speed signal will be used to identify the notch filter width.

IV. Proposed Algorithm

This paper introduces a new algorithm capable of detecting the necessary notch filter width to dampen the resonance in an optimal and efficient manner. It uses the previously identified signal spectrum, which has been introduced in [3]. Due to the implementation on an embedded signal processing platform resource consumption and computing power must be kept to a minimum. The frequency identification was carried out by the "Scanning-Algorithm", which did not use an FFT-based approach due to limited computing power.

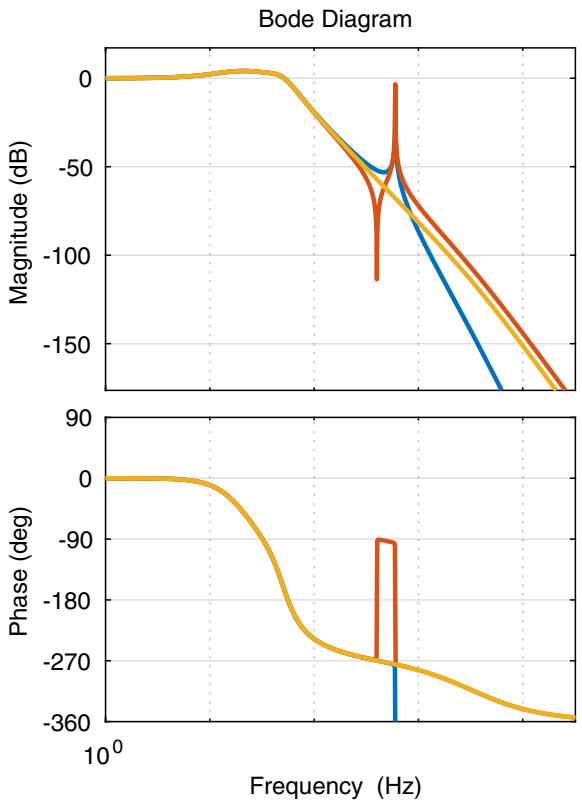

Fig. 2. Bode Plot of different transfer functions of the simulated system with closed loop speed control. The yellow graph represents the rigid coupled system, whereas the load side $G_\mathrm{MA}(s)$ is shown in blue and the $G_\mathrm{MM}(s)$ is shown in red.

A. Algorithmic description

A polynomial function is estimated for the left ($\hat{y}_l(x)$) and right ($\hat{y}_r(x)$) part to the found peak. The peak is described in the point $< x_P/P_P >$. Based on the measured spectrum the surrounding neighborhood of any identified peak shall be equalized and smoothened. Thus, the notch filter width ($\Delta\omega$) needs to determine the point, where the approximated functions are equal to the mean. This yields to:

$$\hat{y}_l(x) = \sum_{n=0}^{N} p_{n,l}\,x^n \tag{12}$$

$$\hat{y}_r(x) = \sum_{n=0}^{N} p_{n,r}\,x^n \tag{13}$$

$$\hat{y}_l(x_{Rl}) = 1 \tag{14}$$

$$\hat{y}_r(x_{Rr}) = 1 \tag{15}$$

$$\Delta\omega = |x_{Rl} - x_{Rr}| \tag{16}$$

The polynomial coefficients $p_{n,[l,r]}$ have to be identified and the order N has to be determined.

Due to the limited computing power, memory and available time the order must not be too big. Choosing

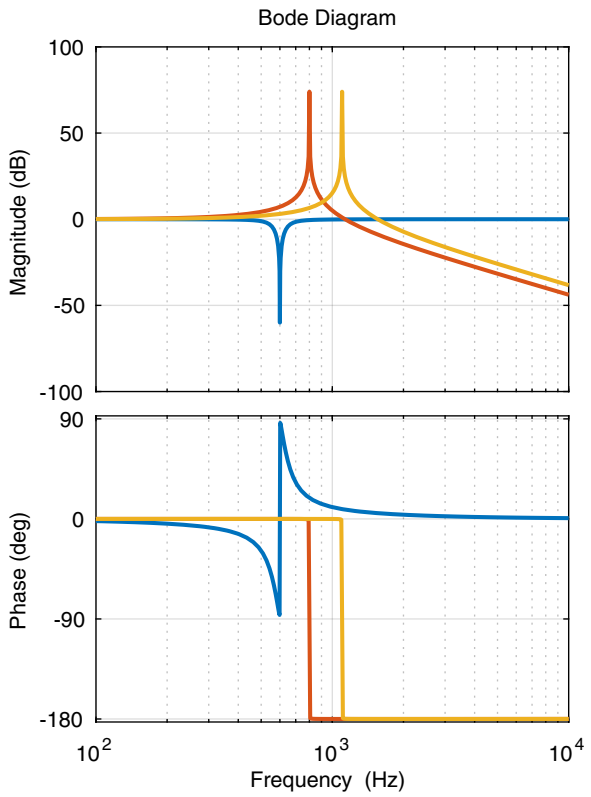

Fig. 3. Bode Plot of additional resonances shown in red and yellow as well as an applied notch filter shown in blue.

$N = 1$ will lead to linear slopes. This yields for x_{Rl} to:

$$x_{Rl} = \frac{1 - P_P}{p_{1,l}} + p_{1,l}\, x_p \tag{17}$$

$$x_{Rr} = \frac{1 - P_P}{p_{1,r}} + p_{1,r}\, x_p \tag{18}$$

$$\Delta\omega = \left| \frac{1 - P_P}{p_{1,l}} - \frac{1 - P_P}{p_{1,r}} \right| \tag{19}$$

$$\Delta\omega = \left| \frac{(p_{1,l} - p_{1,r})(P_P - 1)}{p_{1,l}\, p_{1,r}} \right| \tag{20}$$

Due to the present peak the left slope $p_{1,l}$ must be positive and the right slope $p_{1,r}$ must be negative. This yields to:

$$\Delta\omega = \frac{(p_{1,l} - p_{1,r})(P_P - 1)}{|p_{1,l}\, p_{1,r}|} \tag{21}$$

Equation 21 can be computed efficiently on an DSP since it needs only one division. The next section will deal with the identification of the necessary slopes $p_{1,l}$ and $p_{1,r}$.

B. Identification of polynomial coefficients

Different solutions to this problem are possible. The least square approach would yield to:

$$\underline{b} = \mathbf{A}\underline{x} \tag{22}$$

$$\underline{x} = (\mathbf{A}^T\mathbf{A})^{-1}\mathbf{A}^T\underline{b} \tag{23}$$

$$\mathbf{A}^T = \begin{bmatrix} x_{k-M} & x_{k-M+1} & \dots & x_{k-2} & x_{k-1} \\ 1 & 1 & \dots & 1 & 1 \end{bmatrix} \tag{24}$$

$$\underline{x} = \begin{bmatrix} p_{l,1} \\ p_{l,0} \end{bmatrix} \tag{25}$$

$$\underline{b}^T = [P_{P-M} \quad P_{P-M+1} \quad \dots \quad P_{P-2} \quad P_{P-1}] \tag{26}$$

The parameter $p_{l,1}$ would be the optimal value in a least square sense for considering M points left to the peak. Substituting index r for l would yield to the right side of the peak. The indices x_{P-M} would need to be replaced by $x_{P+1} \dots x_{P+M}$.
Due to weakly dampened peaks the value for M can be approximated as follows:

$$M \approx \frac{50\,\text{Hz}}{\Delta f} \tag{27}$$

A typical value for the frequency step size Δf is 10 Hz. This yields to $M \approx 5$. This leads to a size of $\mathbb{R}^{5\times 2}$ for matrix $\mathbf{A}$ and thus demands memory and resources in the DSP.

Alternatively the mean value of slopes from adjacent points could be calculated. This yields to:

$$\overline{p}_{1,l} = \frac{1}{2\Delta f(M-2)} \sum_{k=M-2}^{1} m_l^*(k) \tag{28}$$

$$\overline{p}_{1,r} = \frac{1}{2\Delta f(M-2)} \sum_{k=1}^{M-2} m_r^*(k) \tag{29}$$

$$m_l^*(k) = (P_{P-k+2} - P_{P-k}) \tag{30}$$

$$m_r^*(k) = (P_{P+k+2} - P_{P+k}) \tag{31}$$

Using $\overline{p}_{1,l}$ and $\overline{p}_{1,r}$ for Equation 21 will lead to the desired results.

C. Improving Robustness of Coefficients

Since the normalized slopes $m_l^*(k)$ and $m_r^*(k)$ can be calculated and stored prior to calculating the mean, this can be used to check the resulting slopes. Since the sign of the slopes must all be positive for $m_l^*(k)$ and negative for $m_r^*(k)$, the slopes with incorrect sign can be discarded.

V. Simulation of Automatic Notch Filter Width

The algorithm will be implemented in MATLAB. The simulation steps include:

1) Stimulating the plant with an PRBS excitation and calculating the power spectrum estimation with the method mentioned in [3].
2) Based on the power spectrum calculate the relative power spectrum as described in [9]. This paper also identified possible resonance peaks, so called candidates.

3) Calculate an estimation for the notch filter width for each candidate:
   a) Calculate the normalized slopes $m_l^*(k)$ and $m_r^*(k)$.
   b) Verify that $\text{sign}(m_l^*(k)) > 0$ and $\text{sign}(m_r^*(k)) < 0$.
   c) Calculate notch filter width $\Delta\omega$ based on Equation 21.

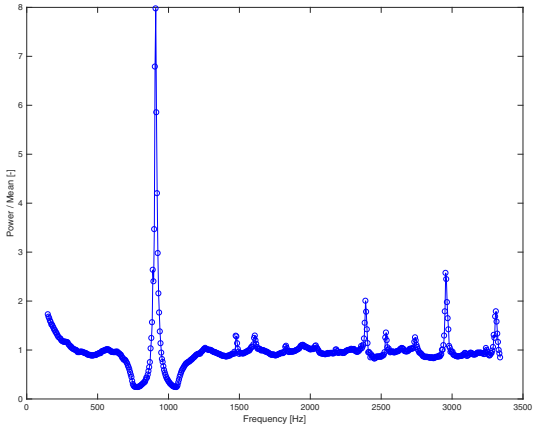

Fig. 4. Estimated relative power spectrum of actual motor speed signal $\dot{\varphi}_M$. This measurement was taken from a machine and three resonances can clearly be seen in this figure and are listed in II.

TABLE II. MEASURED PEAKS ON A MACHINE.

f_{Max} [Hz]	900	2350	2950
P_{rel} [−]	7.9	1.89	2.6
$\Delta\omega$ [Hz]	46	39	45

Figure 4 shows the relative power spectrum identified on a real machine according step one, which will be used during this paper. Three candidates were identified in step two and are listed in Table II.

Figure 5 shows the simulation algorithm of this paper for three peak candidates. It therefore uses the results from Figure 4. The respective peak is indicated with a black diamond. The thick black dashed line represents the average slope to the left and right side of the peak. The horizontal dashed line at height 1 indicates the resulting width. The dotted line in black indicates the threshold for the peak detection, so candidates below the threshold were discarded beforehand.

The red line shows the simulated result when a notch filter with estimated width, depth and resonance frequency was designed and applied to the blue line. It can be seen that the respective peak will successfully be dampened.

VI. CONCLUSION

This paper has used the frequency identification algorithm developed in [3] to detect resonance frequencies present in the mechanical system, which was presented in this paper. Using the detected resonance peaks this paper has introduced a novel and resource efficient algorithm capable of estimating the notch filter width due to limited

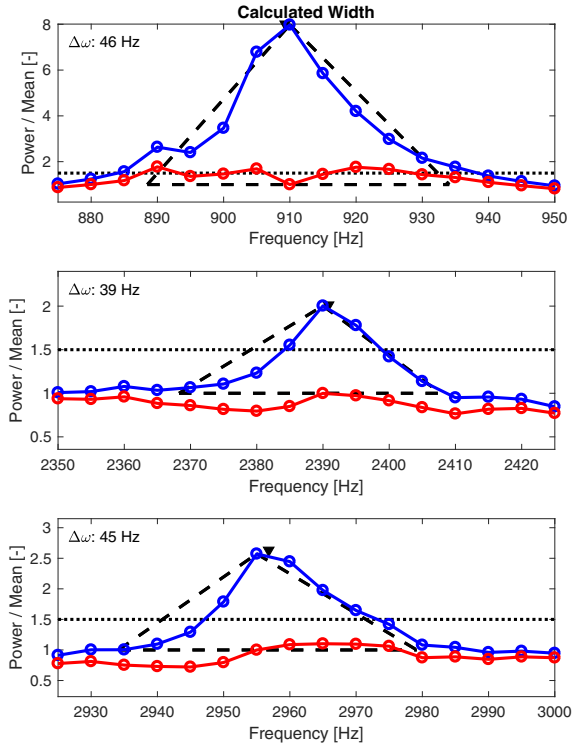

Fig. 5. Identified notch filter width with proposed algorithm. Based on the relative power spectrum (blue) the notch filter width is identified and applied (red). The dashed graph represents the estimated slopes.

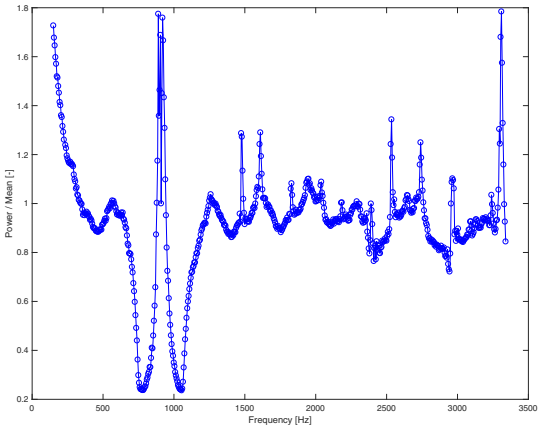

Fig. 6. Estimated power spectrum with applied notch filters. In contrast to Figure 4 the peaks were significantly dampened.

computing power an memory. The algorithm was simulated in MATLAB with measurements from two different machines and valided on a second machine.
Future work will continue to improve robustness of this algorithm for noisy environments.

REFERENCES

[1] F. Mink and A. Bähr, "Adaptive drehzahlregelung bei variablen trägheitsmomenten und eigenfrequenzen," in *SPS IPC DRIVES*, ser.

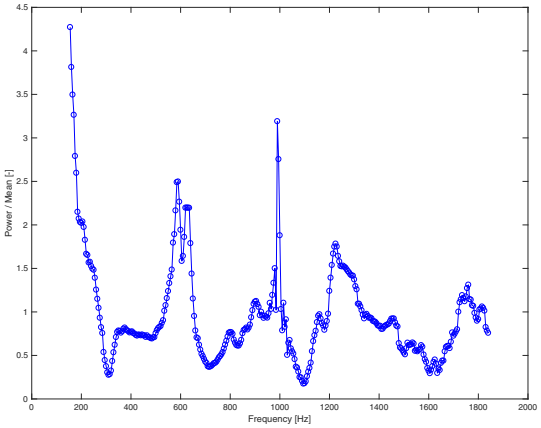

Fig. 7. Estimated power spectrum of actual motor speed signal obtained at a different machine. This measurement will be used to transfer the algorithm to a different dataset.

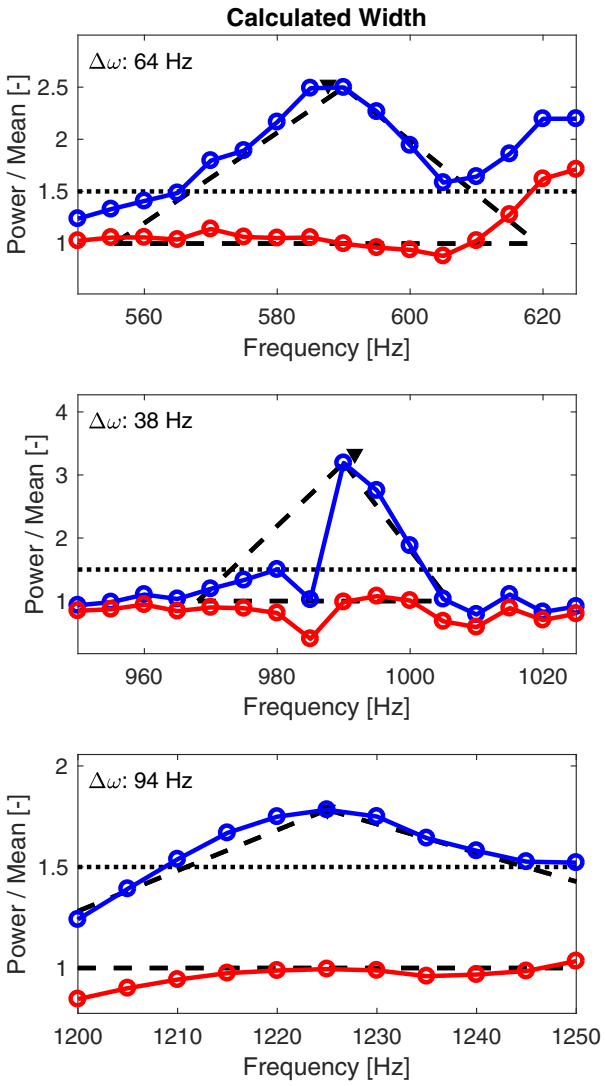

Fig. 8. Identified notch filter width using data from Figure 7. This figure transfers the algorithm to a different machine. The red graph illustrates the filtered data when a notch filter is applied.

SPS IPC Drives, A. Verl, Ed. Berlin: VDE-Verl., 2008, pp. 561–570.

[2] S. Brock, D. Luczak, K. Nowopolski, T. Pajchrowski, and K. Zawirski, "Two approaches to speed control for multi-mass system with variable mechanical parameters," *IEEE Transactions on Industrial Electronics*, vol. 64, no. 4, pp. 3338–3347, 2017.

[3] M. Aldag and J. Horn, "Anwendung adaptiver notch filter bei maschinen mit rotativen direktantrieben," in *Modellbildung, Identifikation und Simulation in der Automatisierungstechnik*, GMA Gesellschaft für Meß- und Automatisierungstechnik, Ed., 2017.

[4] S. E. Saarakkala and M. Hinkkanen, "Identification of two-mass mechanical systems in closed-loop speed control," in *IECON 2013 - 39th Annual Conference of the IEEE Industrial Electronics Society*, IEEE, Ed., 2013, pp. 2905–2910.

[5] J. Weissbacher, E. Grunbacher, and M. Horn, "Automatic tuning of a servo drive speed controller for industrial applications," in *International Conference on Mechatronics (ICM)*, IEEE, Ed., 2013, pp. 700–705.

[6] S. Villwock and M. Pacas, "Application of the welch-method for the identification of two- and three-mass-systems," *IEEE Transactions on Industrial Electronics*, vol. 55, no. 1, pp. 457–466, 2008.

[7] I. Doré Landau, M. Alma, A. Constantinescu, J. J. Martinez, and M. Noë, "Adaptive regulation—rejection of unknown multiple narrow band disturbances (a review on algorithms and applications)," *Control Engineering Practice*, vol. 19, no. 10, pp. 1168–1181, 2011.

[8] M. Yang, H. Liang, and D. Xu, "Fast identification of resonance characteristic for 2-mass system with elastic load," in *International Power Electronics Conference (IPEC-Hiroshima 2014 ECCE-ASIA)*, 2014, pp. 3174–3178.

[9] M. Aldag and J. Horn, "Damping of resonance peaks using adaptive notch filters in gearless servo drives," in *Methods and Models in Automation and Robotics (MMAR)*, 2017, pp. 164–169.

[10] D. Luczak and K. Zawirski, "Parametric identification of multi-mass mechanical systems in electrical drives using nonlinear least squares method," in *IECON 2015 - 41st Annual Conference of the IEEE Industrial Electronics Society*, IEEE, Ed., 2015, pp. 004 046–004 051.

[11] N. Nevaranta, J. Parkkinen, T. Lindh, M. NiemelÃ, O. Pyrhönen, and J. Pyrhönen, "Online identification of a mechanical system in the frequency domain with short-time dft," *Modeling, Identification and Control: A Norwegian Research Bulletin*, vol. 36, no. 3, pp. 157–165, 2015.

[12] R. Neugebauer, A. Hellmich, S. Hofmann, and H. Schlegel, "Non-invasive parameter identification by using the least squares method," *Archive of Mechanical Engineering*, vol. LVIII, no. 2, 2011.

[13] M. Meller, "A self-optimization mechanism for generalized adaptive notch smoother," *Signal Processing*, vol. 129, pp. 38–47, 2016.

[14] D. Luczak, "Delay of digital filter tuned for mechanical resonant frequency reduction in multi-mass mechanical systems in electrical direct drive," in *2015 IEEE European Modelling Symposium (EMS)*, IEEE, Ed., pp. 195–200.

[15] T.-I. Kim, W. Bahn, J.-M. Yoon, J.-S. Han, J.-H. Park, S.-S. Lee, S.-H. Lee, and D.-I. Cho, "Online tuning method for notch filter depth in industrial servo systems," in *Proceedings of the 35th Chinese Control Conference*, J. Chen and Q. Zhao, Eds. Piscataway, NJ: IEEE, 2016, pp. 9514–9518.

[16] D. Borio, "Loop analysis of adaptive notch filters," *IET Signal Processing*, vol. 10, no. 6, pp. 659–669, 2016.

[17] D. Schröder, *Elektrische Antriebe - Regelung von Antriebssystemen*, 4th ed. Berlin and Heidelberg: Springer Vieweg, 2015.

[18] D. Luczak, "Mathematical model of multi-mass electric drive system with flexible connection," in *19th International Conference on Methods & Models in Automation & Robotics (MMAR), 2014*. Piscataway, NJ: IEEE, 2014, pp. 590–595.